

The importance of atmospheric monitoring in Cherenkov experiments

J.L. Osborne, M. Aye, P.M. Chadwick, M.K. Daniel, T.J.L. McComb,
J.M. McKenny, S.J. Nolan, K.J. Orford and S.M. Rayner

Physics Department, University of Durham, South Road, Durham DH1 3LE, United Kingdom.

Abstract. A review is presented of Monte Carlo simulations of the effects of differing atmospheric structure and absorption models on the Imaging Atmospheric Cherenkov Telescope signal. Methods of monitoring the atmosphere are discussed.

Key words: atmospheric Cherenkov telescope, atmospheric absorption, atmospheric monitoring

1. Introduction

The new generation of truly sensitive Atmospheric Cherenkov Telescopes (IACTs) for gamma ray astronomy (Cangaroo-III (Mori 2001), H.E.S.S. (Hofmann 2001), MAGIC (Lorenz 2001), VERITAS (Quinn 2001)) will have high sensitivity, low threshold energy (50 - 100 GeV), arc minute angular resolution and be capable of a good energy resolution of about 15% at most energies. As an instrument for ground-based astronomy, however, an IACT is unique in that the atmosphere is an integral part of the detector system. It is the target medium for the incoming gamma rays and hadrons and the emitting and transport medium for the Cherenkov photons. The atmospheric density profile controls the longitudinal extensive air shower development. The amount of Cherenkov light emitted per unit pathlength of the shower particles and its angle of emission depends on the local refractive index. The amount of light reaching the IACT depends on molecular absorption, Rayleigh scattering by molecules and Mie scattering by aerosol particles and the presence of high altitude clouds. Monitoring of the properties of the atmosphere is therefore essential for the interpretation of the Cherenkov signal in terms of the energy spectrum of the gamma rays and the time variation of source fluxes.

An illustration is given in figure (1) of how the signal recorded by an IACT from 100 GeV gamma ray showers incident at a zenith angle of 30° can depend on the location of the telescope. The simulated mean density of Cherenkov photons as a function

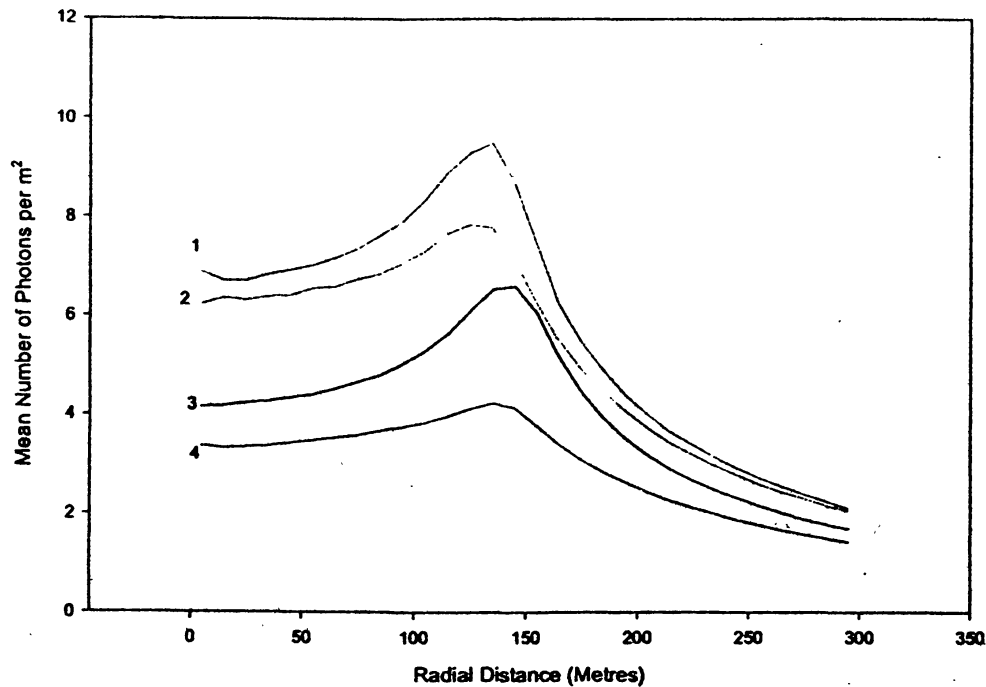


Figure 1. Comparison of lateral distributions of Cherenkov photon density from MOCCA simulations of 100 GeV gamma ray showers for H.E.S.S. (curves 1 and 2) and Narrabri/Woomera (3 and 4) sites, with corresponding geomagnetic fields turned on (2 and 4) and off (1 and 3)

of radial distance from the shower axis is plotted. Curves 1 and 2 are for a 'tropical' atmospheric structure and an altitude of 1800m as appropriate to the H.E.S.S. site in Namibia. Curves 3 and 4 are for a 'U.S. Standard' atmospheric structure and an altitude of 260m to match the former Durham Mk6 site at Narrabri, Australia. (The site of the CANGAROO telescopes at Woomera has similar parameters). The same atmospheric absorption function is used for both. The difference between the even and odd numbered curves shows the effect of the geomagnetic field, which bends the shower particle trajectories and therefore spreads the Cherenkov light distribution. Curves 1 and 3 are for zero field while curves 2 and 4 are for telescope azimuth pointing due South, which, for these southern hemisphere sites, implies that the component of the field perpendicular to the line of sight is near maximum. Due to the geomagnetic field's deviation from a simple dipole the field strength in Australia is nearly twice that in southern Africa.

Our present task to review Monte Carlo simulations of the effects of differing atmospheric properties on the IACT signal is simplified by the fact that, although the various research groups have no doubt produced internal reports on the subject there are few papers in the refereed journals. The most comprehensive account is that of Bernlöhner (2000) and we draw heavily on this and a H.E.S.S. group internal report (Bernlöhner 1998) in the next two sections on atmospheric structure and absorption. In the final section we outline some methods of atmospheric monitoring that the Durham group, as part of the H.E.S.S. collaboration are considering.

2. Atmospheric Structure

The atmospheric density profile affects the longitudinal shower development. For vertically incident 100 GeV gamma ray primaries shower simulations show that the maximum of shower development occurs at a height of about 10 km above sea level when the so-called 'U.S. standard' atmospheric model is used. Atmospheric models which have higher temperatures in the lower part of the atmosphere give maxima at somewhat greater heights.

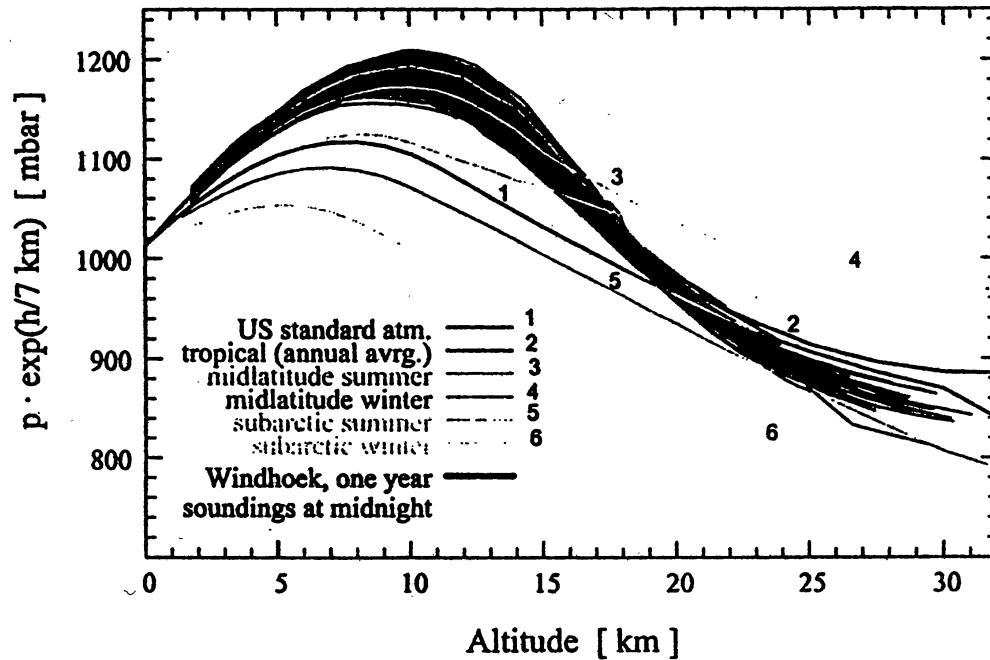


Figure 2. Atmospheric pressure profiles for various built-in MODTRAN models compared with those measured by balloon from Windhoek, Namibia.

Figure 2 shows a set of atmospheric pressure profiles, which may be differentiated to give the density, that are tabulated in the MODTRAN program for atmospheric transmission calculations. Also shown are a whole year's radiosonde soundings from Windhoek, Namibia. It can be seen the 'Tropical (annual average)' curve fits these data well. As is to be expected the seasonal variation in the profiles increases with geographic latitude.

The Cherenkov efficiency in terms of the number of photons between wavelengths λ_1 and λ_2 emitted by a particle of charge z per unit pathlength, $\frac{dN}{dx}$, and its angle of emission, θ_c , depends on the local refractive index $n(\lambda)$.

$$\frac{dN}{dx} = 2\pi\alpha z^2 \int_{\lambda_1}^{\lambda_2} \left(1 - \frac{1}{(\beta n(\lambda))^2}\right) \frac{1}{\lambda^2} d\lambda \quad (1)$$

where α is the fine structure constant.

$$\theta_c = \arccos(1/n\beta) \approx \sqrt{2(n-1)} \text{ radians} \quad (2)$$

in simulations $n-1$ is usually taken to be simply proportional to air density and its 5% variation with λ over the 300-650 nm sensitivity range of photomultipliers is ignored.

The lateral distribution of Cherenkov light at ground level from gamma ray showers is determined mainly by the emission angle and its height of production. At height $h = 10\text{km}$ above sea level the atmospheric density is such that $\theta_c \approx 0.014\text{radians}$ and the light thus falls on a ring of about 140 m radius. An approximate compensation of the reduction of θ_c with increasing h over an 8-16km height range leads to 'focussing' of the light into a characteristic ring of near constant radius as can be seen in figure 1. Multiple Coulomb scattering gives an angular and lateral spread of the charged shower particles which tends to fill in the ring and this effect is enhanced by the light from particles below the median height of emission. From (1) it can be seen that the Cherenkov efficiency at the median height of emission, h_{med} is proportional to the square of the corresponding Cherenkov angle θ_{med} while the light is spread over a pool of approximate area $\pi\theta_{\text{med}}^2(h_{\text{med}} - h_{\text{obs}})^2$ at the height of observation, h_{obs} . Thus the central light density for vertical showers, ρ_c , ignoring absorption, follows

$$\rho_c \propto \frac{1}{(h_{\text{med}} - h_{\text{obs}})^2} \quad (3)$$

The effect of this on the lateral distribution of Cherenkov light photons is shown in figure 3. In the extreme cases the antarctic winter profile gives 60% more light than the tropical one. For sites at moderate latitudes the seasonal effect of 15-20% is important to consider as is the effect of different atmospheric profiles when cross calibrating IACTs on, for instance, the Crab nebula.

3. Atmospheric absorption

The amount of light reaching the IACT depends on

- a Molecular absorption,
- b Rayleigh scattering by molecules,
- c Mie scattering by aerosol particles.

The molecular and aerosol scattering is generally treated as an absorption process. Bernlöhner shows that the fraction of light scattered into the viewing angle within the typical ($\sim 25\text{ns}$) integration time of an IACT is no more than a few percent. The wavelength dependence of the absorption by the various components of the atmosphere is shown in figure 4.

Photomultipliers with borosilicate glass windows are sensitive in the 290 to 650nm wavelength range. Here the majority of the attenuation is due to Rayleigh scattering

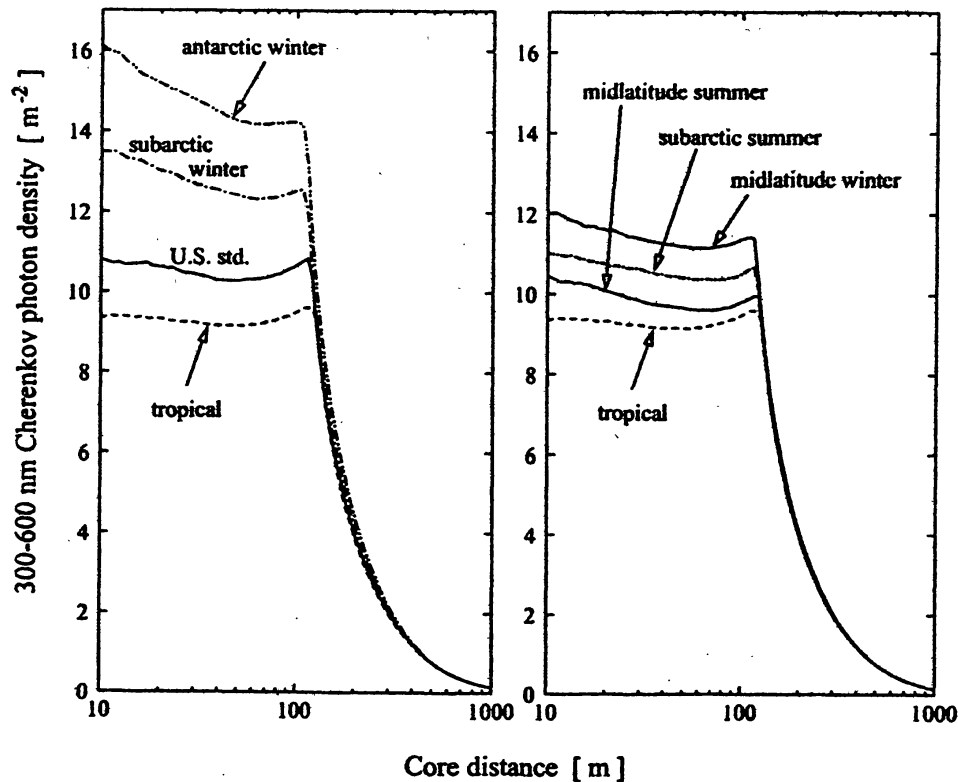


Figure 3. The average lateral distributions of Cherenkov photons (300-600nm) at 2200m a.s.l. for vertical 100GeV gamma ray showers from CORSIKA simulations with different atmospheric profiles. The same absorption model (U.S. Standard profile with rural haze is used for all). (Bernlöhr 2000)

from air molecules. This scattering is easily predictable and shows only small temporal variation. Mie scattering by aerosols is more complex and depends on the size, shape and composition of the particles. It is almost independent of wavelength. Aerosol density is site and time dependent. The height and thickness of aerosol layers may vary although they will generally be found in a boundary layer extending to 1 or 2km above the ground. Stratospheric aerosol clouds may also be present, typified by the Sahara dust clouds that appear over the La Palma site or the input from volcanic activity. Figure 5 shows a distribution of aerosols which is largest within a few kilometers of ground level but also shows the effect of a strong component of stratospheric volcanic dust.

Molecular absorption is mainly due to ozone. The ozone concentration is also site and time dependent and is not necessarily concentrated at high altitudes. The absorption cuts in very sharply below 330 nm. The use of photomultipliers whose sensitivity extends into the ultraviolet enhances the Cherenkov signal but makes it more liable to variations in the ozone levels.

As can be seen in figure 4 gaseous water vapour plays only a minor part in molecular absorption. It affects only wavelengths longward of 550nm, in the tail of the photomultiplier sensitivity curve, and even here the effect is small. Precipitable water vapour

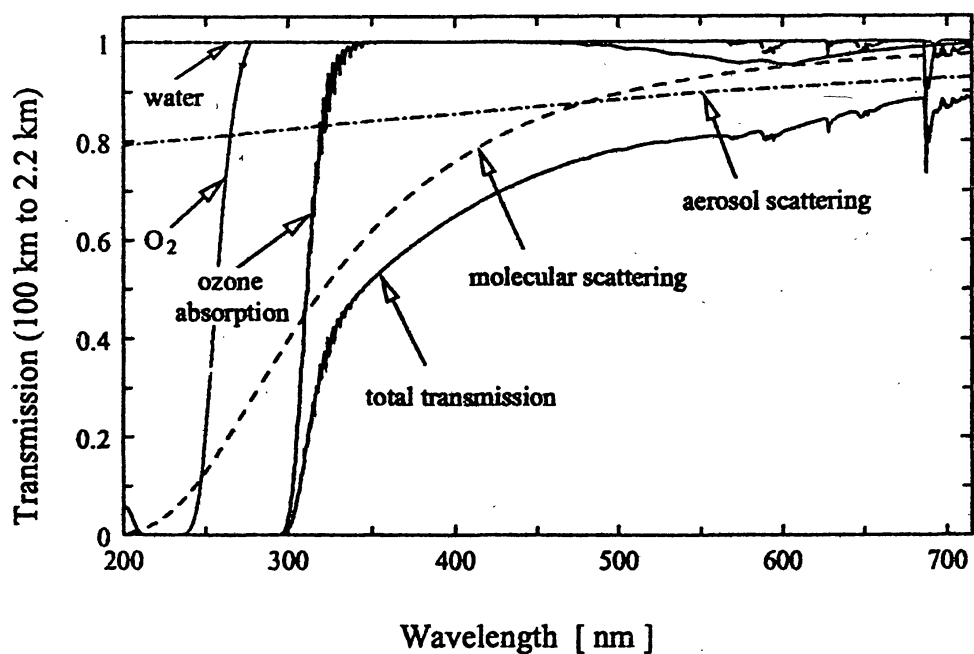


Figure 4. The atmospheric absorption from space to the HEGRA altitude (2200m) for the various absorbing processes. (Bernlöhr 2000)

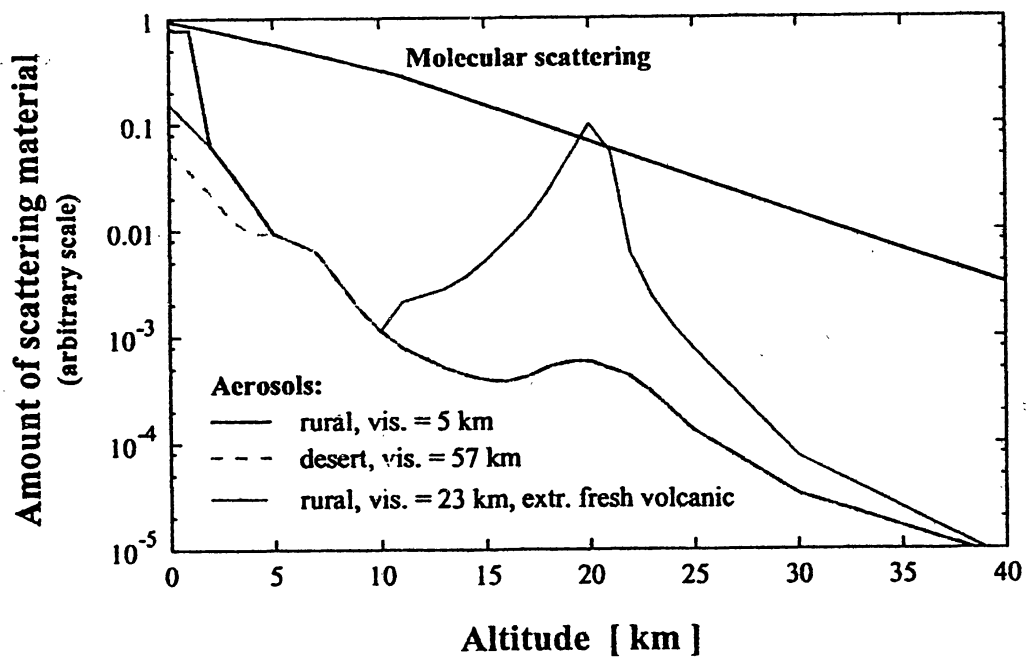


Figure 5. Vertical atmospheric profiles of the amount of scattering material for molecular scattering (proportional to air density) and aerosol scattering for different MODTRAN aerosol models (Bernlöhr 1998).

in the form of droplets with sizes comparable to and larger than the wavelength of the light is, of course, important and can manifest as haze or thin high cloud. Water vapour coalescing on aerosols affects their scattering properties.

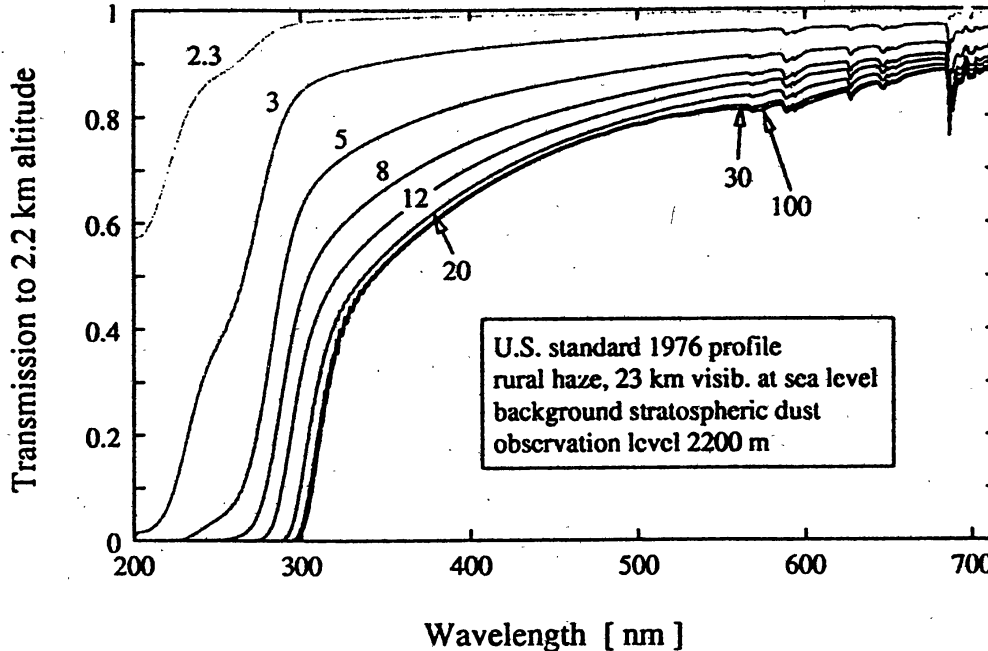


Figure 6. Transmission of light along vertical paths from various altitudes (in km) to an observation level of 2.2 km. Transmission was calculated with MODTRAN for the parameters shown in the box. (Bernlöhr 2000)

The MODTRAN program enables tables of atmospheric transmission to be calculated when the distribution of the various absorbing components has been chosen. Figure 6 shows such a table plotted for light arriving at an observation level of 2200 m.

4. Atmospheric monitoring

From what we have already indicated it is clear that the following atmospheric profiles need to be monitored.

- a. Pressure and temperature.
- b. Precipitable water vapour.
- c. Aerosols.
- d. Ozone.

The established method of measuring atmospheric pressure and temperature is by the use of radio sondes on free flying balloons which give data up to 30 km. Off-the-shelf systems are available at moderate cost. It may well be that data from the nearest government meteorological station will be sufficiently well correlated with on site measurements

to make continued local flights redundant. Tethered systems which can sample up to 3 km, where local variations may be largest, have a reduced capital and ongoing cost.

Water vapour profiles can be measured with radio sondes. The Durham group has had extensive experience of using commercial MIR radiometers working in the 8-14 μm band (Buckley et al. 1999). These give a measure of the integrated water vapour profile. Figure 7 illustrates the straightforward application of such a radiometer as a passive cloud detector. This was attached to the Narrabri Mk 6 IACT to monitor the temperature in its FOV. This temperature is very sensitive to the presence of clouds on account of their being warmer than the clear sky background. The effect of the passage of a small cloud through the FOV is to give a strong anti-correlation of temperature and the IACT counting rate.

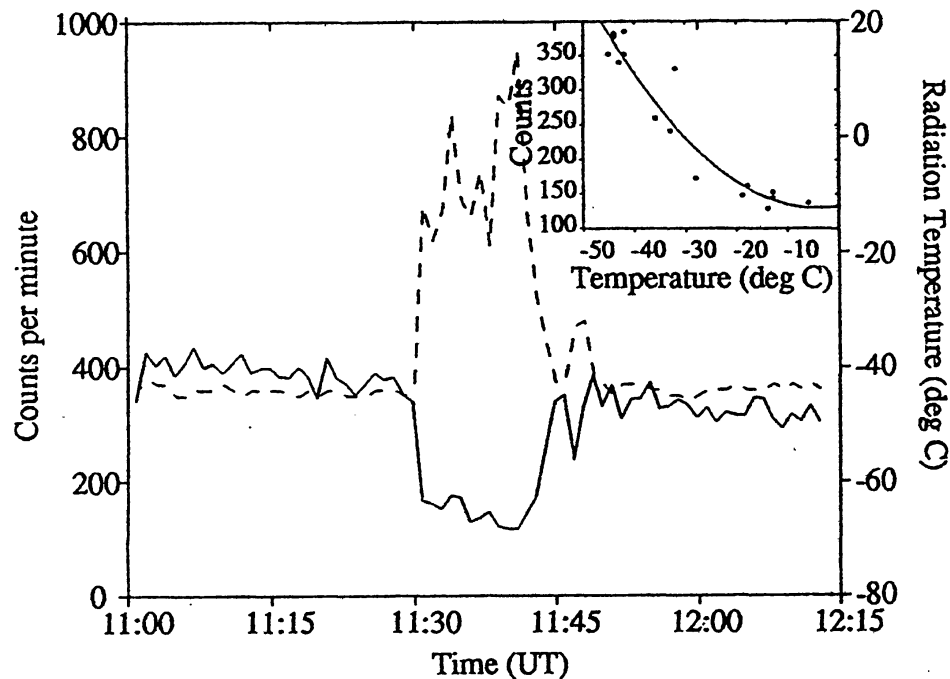


Figure 7. An example of the correlation between the background counting rate of the Narrabri Mk 6 IACT and the radiation temperature of the sky as measured by a Heimann model KT17 MIR radiometer. The main figure shows the time variation of the IACT counting rate (solid line) and the radiative temperature (broken line). The inset shows the correlation. (Buckley et al. 1999)

Aerosol profiles can be obtained from commercial cloud-sensing LIDAR systems. Typically these may use an InGaAs pulsed laser operating at 905 nm or a Nd:YAG laser at 532 nm. In practice a mixture of water vapour and aerosol profiles may be obtained and the aerosol profile needs separating by another water detection method. Aerosols in the possibly important ground boundary layer needs monitoring by use of a stabilised, filtered light source on a remote hill top. It may be possible to correlate local aerosol measurements with satellite data (e.g. TOMS).

Measurement of the real time ozone profile requires differential multiwavelength absorption LIDAR operating in the 200-300 nm region. This could be expensive but one should bear in mind that the necessary elements of such a system in addition to the UV laser are a large steerable optical receiver and a fast optical detector package with digitization and recording facility which are provided by the IACT itself.

5. Conclusion

It has been shown how the atmosphere is an integral part of the whole IACT detection system and that the monitoring of its properties is therefore essential for the interpretation of the Cherenkov signal in terms of the energy spectra and time variation of very high energy gamma ray sources. One important method of monitoring not yet mentioned is via the trigger rate from the much more numerous hadronic cosmic ray showers. This gives a 'direct' measurement of the sum of all the effects of temporal variations of the atmosphere on the Cherenkov light. Because of the differences in the development of the showers and the contribution from penetrating muons extensive Monte Carlo simulations are needed for good quantitative interpretation.

References

- Aye, M., Chadwick, P.M., Daniel, McComb, T.J.L., McKenny, J.M., Nolan, S.J., Orford, K.J., Osborne, J.L. and Rayner, S.M., 2001, Proceedings of ICRC 2001, Copernicus Gesellschaft, p.2859.
- Bernlöhner, K., 1998, HEGRA/HESS Internal Report, CORSIKA and SIM.TELARRAY, Chpt 6.
- Bernlöhner, K., 2000, *Astroparticle Physics*, 12, 255.
- Buckley, D.J., Donnington, M.C., Edwards, P.J., McComb, T.J.L., Tummey, S.P. and Turver, K.E., 1999, *Experimental Astronomy*, 9, 237.
- Hoffmann, W., 2001, Proceedings of ICRC 2001, Copernicus Gesellschaft, p.2785.
- Lorenz, E., 2001, Proceedings of ICRC 2001, Copernicus Gesellschaft, p.2789.
- MODTRAN patented software, US Air Force Phillips Laboratory, www-vsbn.plh.af.mil/soft/modtran4.html
- Mori, M., 2001, Proceedings of ICRC 2001, Copernicus Gesellschaft, p.2831.
- Quinn, J., 2001, Proceedings of ICRC 2001, Copernicus Gesellschaft, p.2781.